Rheol Acta (2004) 44: 38–46
DOI 10.1007/s00397-004-0370-y

ORIGINAL CONTRIBUTION

Lei Li
Hua Hu
Ronald G. Larson

DNA molecular configurations in flows near adsorbing and nonadsorbing surfaces

Received: 25 September 2003
Accepted: 17 January 2004
Published online: 4 June 2004

L. Li · H. Hu · R. G. Larson (✉)
Department of Chemical Engineering,
University of Michigan,
Ann Arbor, MI 48109, USA
E-mail: rlarson@engin.umich.edu

Present address: L. Li
Dept of Pharmaceutical Sciences,
University of Michigan,
Ann Arbor, MI 48109, USA

Abstract We investigate experimentally λ-phage and T2-coliphage DNA molecules near both nonadsorbing glass and adsorbing 3-aminopropyltriethoxysilane (APTES)-coated glass surfaces in a simple steady shearing flow generated by a torsional flow cell. The DNA molecular deformations near the surface are found to be considerably weaker than in bulk flow at the same shear rate. This affects the DNA molecule's deposition and stretching on the adsorbing surface. Surprisingly, for a simple shearing flow in the torsional shearing device, the observed stretch, for molecules both near (< 10 μm) the surface and adsorbed to it, is much less than predicted by simulations.

Keyword Shearing flow · DNA molecule · Glass surface · Bulk and surface behavior · Molecular deformation

Introduction

Recently there have been numerous studies of DNA molecular motion and deformation induced by viscous flows, magnetic fields, electric fields, and electroosmotic flows.. Because DNA not only carries genetic information, but is also a macromolecule large enough to be visualized optically, its physical behavior under flow and other fields can provide us insights into polymer physics at the molecular level.

So far, experimental and theoretical studies of single-molecule DNA dynamics in flow fields have yielded a reasonably thorough understanding of their behavior in the bulk (Perkins et al. 1997; Smith and Chu 1998; Smith et al. 1999; Babcock et al. 2000; Larson et al. 1997, 1999; Hur et al. 2000). With the rapid growth of genetic analyses, there is also an increased interest in DNA molecular behavior near solid surfaces or in a confined geometry, which is much less understood than the bulk behavior of DNA in flow. Possible applications include DNA separation using confinement effects (Han et al. 1999; Han and Craighead 2000; Doyle et al. 2002; Jendrejack et al. 2003) or using electrophoretic movement on flat surfaces (Pernodet et al. 2000). In addition, DNA stretching and deposition onto an adsorbing surface (Bensimon et al. 1994, 1995; Hu et al. 1996; Allemand et al. 1997; Yokota et al. 1999; Abramchuk et al. 2001; Klein et al. 2001) has been used to enable subsequent gene mapping by restriction digestion or hybridization (Schwartz et al. 1993; Michalet et al. 1997; Cai et al. 1998; Gad et al. 2001).

Recently, the Schwartz group (Jing et al. 1998) has developed a method for optical mapping of DNA molecules that have been stretched and deposited onto a substrate by the flow in an evaporating sessile droplet. The flow field induced by the evaporation drags the

DNA molecules towards the substrate and the edge of the droplet. DNA molecules deposit onto the glass surface and are stretched in the radial direction.

The glass surface is treated with 3-aminopropyltriethoxysilane (APTES), rendering it positively charged, so that DNA will adsorb to it. The better the stretching of the DNA molecules, the easier the subsequent optical mapping, which uses restriction digestion with endonucleases and optical measurement of the position of the restriction digestion points along the contour of the deposited DNA molecules. This method can be used for high-throughput gene analyses.

The development of methods such as these has highlighted the need for an improved understanding of the interaction of flowing polymer molecules with surfaces. Here, we study DNA deformation on and near surfaces in a simple torsional steady shearing flow produced between two parallel disks by rotation of one of the disks about an axis normal to the disks. Other studies have focused on polymer concentrations near surfaces under flow and are reviewed in our recent theoretical paper (Chopra and Larson 2002).

In the following section we introduce our experimental setup and procedures; following that we discuss the results obtained in a simple steady shearing flow. Finally, we present our conclusions.

Experimental setup and methods

Glass surface treatment Glass coverslips (Corning No.1, 25 mm square) were prepared using the method adopted from Jing et al. (1998) and described in detail in Chopra et al. (2003). Briefly, the coverslips were cleaned by boiling in concentrated nitric acid HNO_3 for 7 h, followed by boiling in 6 N hydrochloric acid HCl for 4 h. The glass coverslips were rinsed thoroughly with de-ionized water, making them ready for APTES coating. In a glove box with N_2 blowing in to control humidity which affects hydrolysis, a 2 vol.% APTES aqueous solution was prepared, and we added 100 ppm of the 2% APTES aqueous solution to ethanol immediately, and hydrolyzed for 7 h. Then we incubated clean cover slips in APTES/ethanol for 48 h in the glove box filled with N_2, and aged the coverslips in desiccators in a refrigerator for about one to seven days.

Stained DNA solutions We used 54%, 60%, and 66 wt% sucrose sugar solutions, with 50 pg/μl 48.5-kbp λ-phage DNA (New England BioLab) stained with YOYO-1 fluorescent dye (Molecular Probe Inc.) at a dye-to-base-pair molar ratio of 1:8, and 10% β-mercaptoethanol (Sigma). The solution contained 10 mmol/l tris-HCl and 1 mmol/l EDTA at pH 8.0. For each experiment in torsional simple steady shearing flow, 200 ml of solution was put onto the glass coverslip, the gap between the upper motor-driven plate and the lower coverslip holding the solution was adjusted, and then the flow was immediately started.

Image acquisition and analysis Stained DNA molecules either in bulk solution or on the coated glass slips are visualized using a Nikon TE200 fluorescent microscope with a 100× oil immersion objective with N.A (numerical aperture) of 1.4 and focal depth of 0.6 μm, with a digital interline CCD camera MicroMax 1300YHS (Princeton Instruments, distributed by Fryer Co.) to capture both still and dynamic images at a resolution of 1300×1030 using full-chip acquisition. The image acquisition software MetaView/MetaMorph version 4.5 (Universal Image, distributed by Fryer Co.) is used to control the camera, the XYZ stage motor (Prior Inc.), and the electronic shutter (Uniblitz VMM-D1, Vincent Associates), and to run the image analysis software. The exposure time is about 50 ms for images taken near the surface ($H < 10$ μm) to 20 ms for bulk positions, which is much larger than 10 s, the time for DNA molecule diffuse out of the depth of focus.

Equipment setup The torsional flow cell is mounted on the motorized stage of the microscope and the upper plate is rotated by a motor. The lower plate is a replaceable glass coverslip. The dimensions of the flow cell are 1 cm in diameter and a height that is adjustable from 0 to 5000 μm by moving the upper plate. In our experiments, we keep the gap at 500 μm. Figure 1 is a close-up view of the torsional flow cell.

Alignment of the plates in the torsional shearing flow cell To align the plates, we mark four pairs of points which are at the corners of a square with a diagonal of 8 mm. A similar set of four points is marked on both upper and lower plates with each point on the upper

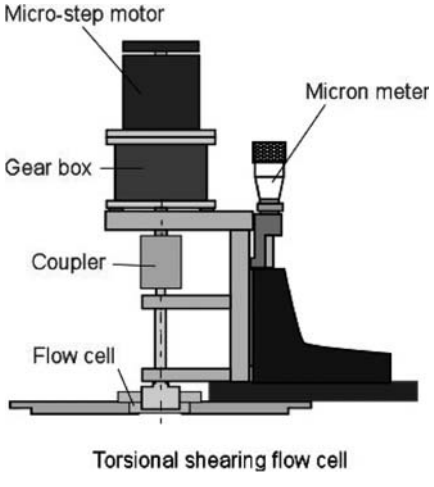

Fig. 1 Torsional shearing flow cell

plate at same x-y position as the corresponding point on the lower plate. We lower the upper plate and allow it gently to touch the lower plate, possibly at an angle if the plates are not parallel. Using adjustable screws for the upper plate on the flow cell we bring all eight points on the upper and lower plates into the same focal plane using a 20× objective whose depth of focus is 10 μm. Then, to confirm the parallelism of the plates, we raise the upper plate so that the gap is about 100 μm, as determined by the micrometer attached to the upper plate, and measure the gap again at each of these four positions by focusing on each of the pairs of markers on each of the four positions. If we find the tilt angle between the two plates to be less than 0.1°, we consider the alignment to be acceptable. Detailed particle image velocimetry (PIV) measurements of the flow field were performed and these confirmed that a uniform simple shearing flow was generated by the flow cell (Hu and Larson 2002).

Results and discussion

Steady torsional shear flow

We performed experiments with dilute λ-phage and T2-coliphage DNA solutions in the torsional flow cell described above. The viscosities of these DNA sugar solutions are given in Table 1. If not mentioned, the results shown are from the 60% sugar solution.

DNA stretching in bulk solutions

First, we determine the relaxation time of the DNA molecules as a function of sugar concentration. We shear at high speed (3.8 rpm) and abruptly stop the flow to allow the stretched DNA chains to relax, and plot x^2, the stretch length squared of the chain vs time. The relaxation time of a DNA chain is determined by fitting the last portion of the curve corresponding to values of x that are less than 30% of L, the fully extended contour length of DNA, with a single exponential function (Larson et al. 1999):

$$\langle x^2(t)\rangle = Aext\left(-t/\tau_{\exp}\right) + B \tag{1}$$

where A and B are fitting parameters, and the brackets $< >$ represent an average over 10 to 20 molecules.

We can also calculate the longest relaxation time of DNA molecules in these solutions using the Rouse model (Larson et al. 1999), which is

$$\tau_R = \frac{\varsigma^R_{total}\langle R^2\rangle}{6\pi^2 k_B T} \tag{2}$$

where ζ_{total} is the drag coefficient for the whole molecule. Here, we calculate this drag coefficient from the Batchelor formula for the drag on a slender cylinder (Li et al. 2000; Li and Larson 2000b) $\varsigma^R_{total} = \eta_s \frac{2\pi L}{\ln\left(\frac{L}{d}\right)}$ with η_s the solvent viscosity and d the diameter of the DNA chain, which is 2 nm for DNA (Pecora 1991). For DNA, which is a semi-flexible worm-like chain, the equilibrium end-to-end distance in the rest state, $< R^2 >_{\text{o}}$, can be calculated as $< R^2 >_{\text{o}} = 2\lambda_{\text{p}} L$. Here, λ_{p} is the molecular persistence length, which is around 0.066 μm for λ-phage DNA stained with YOYO dye (Quake et al. 1997), and L is the contour length of the molecule, which is $L = 21$ μm. k_B is the Boltzmann constant, and T is the temperature in K. Then Eq. (2) can be written as

$$\tau_R = \frac{\langle R^2\rangle_0 L\eta_s}{9.42\ln(L/d)k_B T} \tag{3}$$

The longest relaxation time can also be calculated from the Zimm model for a theta solvent, giving (Doi and Edwards 1986; Li and Larson 2000b):

$$\tau_Z = \frac{[\eta]_0 M\eta_s}{S_1 N_A k_B T} = \frac{\Phi\langle R^2\rangle_0^{\frac{3}{2}}\eta_s}{S_1 N_A k_B T} = \frac{[\eta]_0 M\eta_s}{\frac{S_1 N_A}{\Phi} k_B T} \tag{4}$$

where $N_A = 6.023\times10^{23}$, $S_1 = 2.236$, and $\Phi = 2.2$–2.87×10^{23}; hence $\frac{S_1 N_A}{\Phi} = 5.02 - 6.49$.

Table 1 Relaxation time s of λ-phage and T2-phage DNA solutions at different concentrations of sugar

DNA	Sugar conc. (wt%)	η_s Pa s	τ_Rs	τ_Z s	$\tau_{\exp}$ s	errτ (%)	λ_p μm	L μm
λ-phage		0.014	2.208	2.354	2.18 ± 0.18	1.26	0.066	21
	54							
	60	0.061	9.963	10.622	9.06 ± 0.58	9.07		
	66	0.210	34.174	36.434				
T2-phage	60	0.061	90.646	64.167			0.066	67.2

$\tau_R$is calculated from Eq. (3)
$\tau_Z$is calculated from Eq. (4) using $\frac{S_1 N_A}{\Phi} = 6.49$
$\tau_{\exp}$is obtained by fitting the square of the DNA stretch vs time from Eq. (1)
The viscosities are measured at 20 °C and concentrations of the sugar are approximate

The relaxation times obtained from these two formulas and from the experimental measurements are listed in Table 1. This shows that the longest relaxation times calculated from the Rouse model are very close to the experimental results; the deviation is around 10%. Note that for λ-phage DNA, the Zimm relaxation time τ_z calculated using the largest value of $\frac{S_1 N_A}{\Phi} = 6.49$ is actually larger than the Rouse relaxation time, τ_R. This occurs because for λ-phage DNA, the quantity $\frac{L}{\ln(L/d)}$ is scarcely larger than $\langle R^2 \rangle_0^{1/2}$; for longer DNA molecules, such as T2 DNA, $\frac{L}{\ln(L/d)}$ becomes larger than $\langle R^2 \rangle_0^{1/2}$, and $\tau_R > \tau_z$. In a previous paper (Hsieh et al. 2003), we showed in detail that the effect of hydrodynamic interactions is very weak in dilute λ-phage DNA solutions, which is consistent with the fact that τ_R is not larger than τ_z. Since it is difficult to obtain the relaxation time of DNA in a very viscous solution without precipitation of the sugar in 66% sugar solution, we therefore define the Weissenberg number, $Wi = \tau\dot{\gamma}$, using the "Rouse" longest relaxation time, τ_R, calculated from Eq. (3). The relaxation times measured from these experiments are in the range of reported values for λ-phage DNA from other experiments (Perkins et al. 1997; Smith and Chu 1998; Babcock et al. 2003).

After determining the longest relaxation time of the DNA molecules in solutions with different concentrations of sugar, we measured the DNA molecule's average stretch length $< x >$, which is the average of the maximum stretched length, in bulk solutions (around 20 μm away from the glass surface) at different shear rates. We took snapshots at different radial positions, which have different values of Wi, then analyzed the average stretch ratio $< x/L >$ over 1000 molecules at each Wi, and compared our results to those of the group of Chu and coworkers (Smith et al. 1999). Our results for the average stretch ratio $< x/L >$ vs Weissenberg number Wi (see Fig. 2) in bulk solution under steady shear are in very good agreement with the results of the Chu group, which were obtained in a sliding-plate geometry. This indicates that DNA molecules have similar behavior in steady simple shearing flow generated either by the torsional flow cell or by a sliding plates.

DNA stretching near clean glass surfaces

Next, we took images of DNA molecules at different heights H above the lower glass surface, and plotted the average stretch ratio $< x/L >$ vs Weissenberg number Wi at $H = 1$ μm, 3 μm, 5 μm, 7 μm, 10 μm from the wall, and in the bulk solution, which is around 20 μm from the wall (see Fig. 3). Evidently, the average stretch ratio close to the wall is much smaller than that in the bulk. Figure 4 plots the average stretch ratio $< x/L >$ vs

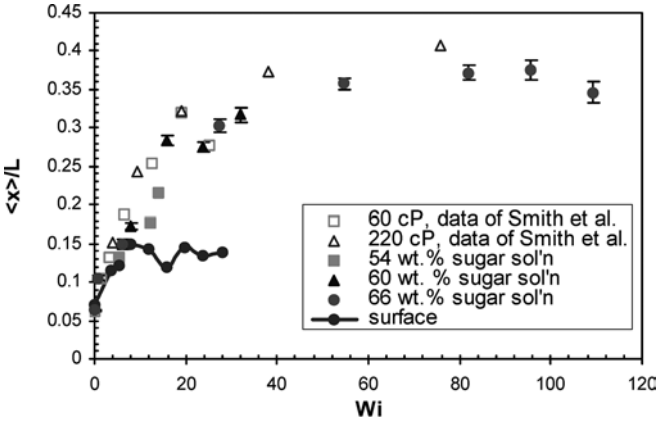

Fig. 2 λ-Phage DNA average stretch ratio $< x/L >$ vs Weissenberg number Wi in bulk solution in three different sugar concentration solutions (*solid squares* represent the results in 54 wt% sugar, *solid triangles* in 60 wt% sugar, and *solid circles* are in 66 wt% sugar) compared to the results obtained in a sliding-plate device by Smith et al. (1999) and to stretch of DNA adsorbed onto an APTES-coated surface at 60 wt% of sugar

the dimensionless distance from the wall H/L. Surprisingly, Fig. 4a shows that the average stretch ratio increases linearly with H in the near-wall region where the dimensionless distance H/L is less than 1/3, and approaches bulk behavior when H/L is equal to or greater than about 1/3, namely 7 μm for λ-phage DNA.

In order to check the scaling of this phenomenon with molecular contour length, we performed similar experiments with T2 DNA (Sigma-Alderich), which has 164 K base pairs and a contour length $L_{T2} = 67$ μm, about three times greater than that of λ-phage DNA ($L_{\lambda\text{-phage}} =$ 21 μm). Again, the longest relaxation time, τ_R, of T2-phage DNA in 60 wt% sucrose solution is calculated by

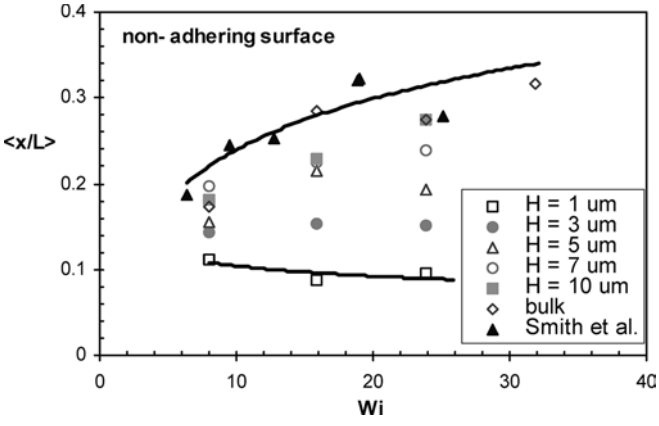

Fig. 3 The average stretch ratio $< x/L >$ of λ-phage DNA molecules vs Weissenberg number Wi in the bulk and the near-wall regions for a non-adsorbing glass surface. The *error bars* are the size of the data symbols or smaller. The lines are for bulk and M = 1 μm, to guide the eye

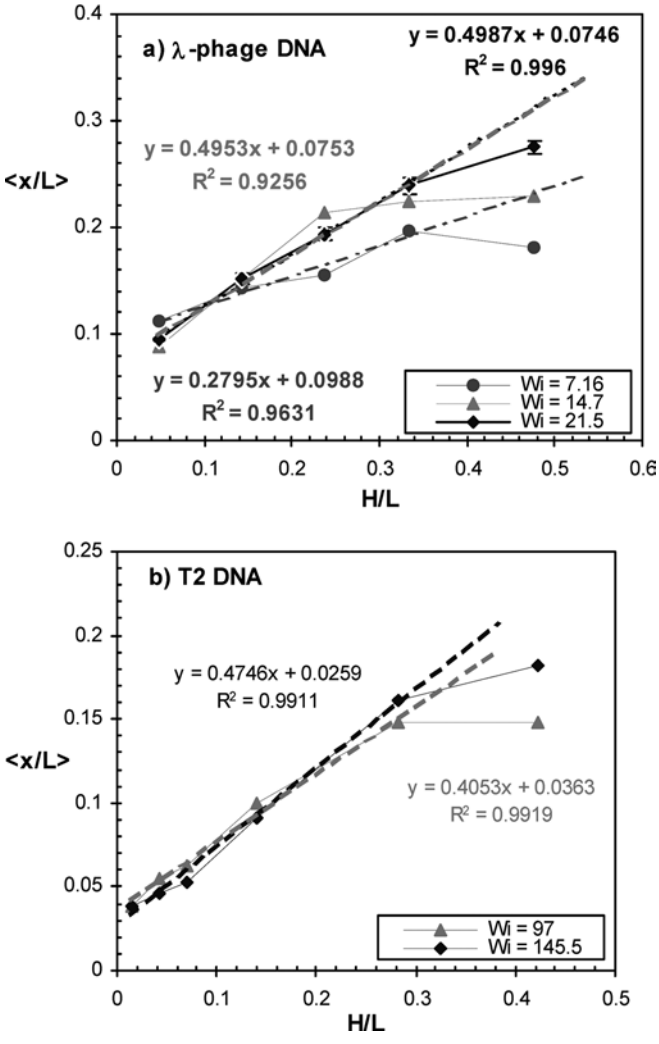

Fig. 4a,b Average stretch ratio of DNA molecules $< x/L >$ vs dimensionless distance from the wall H/L for non-adsorbing surfaces: **a** λ-phage DNA molecules; **b** T2 DNA molecules. *Symbols* are experimental data and *dashed lines* are linear fits of the trends

Eq. (3), and it is listed in Table 1. In Fig. 4b, which shows the average stretch ratio vs the dimensionless distance from the wall for T2 DNA, the slope of the curve is about the same as for λ-phage DNA, namely around 0.45, and the distance at which bulk behavior is attained is again about 1/3 of the contour length L. Therefore, we conclude that DNA molecules experience significant restrictions on stretching in the near-wall region, which is defined as $H \leqslant \frac{1}{3}L$.

We did not observe any instances of molecular breakage or other artifacts that might affect our results. Nevertheless, to confirm that the dependence of stretch on distance H from the wall is not an experimental artifact, we analyzed the integrated light intensity of each object (that is, each individual DNA molecule in each image) to determine whether the DNA molecules near the surface were less bright, and therefore contained less mass, than DNA molecules in the bulk. The measurement of DNA light intensity involves three steps, first the identification of pixel groupings, so-called regions of interest (ROI) that correspond to individual DNA molecules, second the determination of total normalized light intensity of each ROI, and third the measurement of the stretched length of the molecule. The first step is accomplished first by setting a threshold light intensity, chosen to be 15–50 for 8-bit images depending on the exposure time of the images, which for each image is chosen to be slightly greater than the background light intensity of DNA-free regions of the image which have intensities of 10–45. All pixels exceeding the threshold are considered to be "occupied" by a DNA molecule. Next, "occupied" pixels that are contiguous to each other are assigned to be same DNA molecule and called Regions of Interest (ROI). This step is valid for sufficiently dilute solutions, such as those used here, where DNA molecules rarely overlap each other in the image. After identifying the ROIs, each ROI was inspected visually to identify and remove from consideration bright spots due to camera readout noise that were clearly not single DNA molecules, as well as fragmented DNA images whose middle sections are out of the depth of focus, and overlapping DNA molecules. These anomalous, rejected ROIs represent fewer than 10% of total DNA molecules in all processed images. This completes step one, the identification of each group of pixels that corresponds to a DNA molecule.

To accomplish step two, we added up the light intensity of all pixels in each ROI, to give a quantity that is proportional to the mass of that molecule (since the dye stains the molecule uniformly). Because images might differ from each other in illumination conditions (since, as mentioned above, we use different exposure times at different distance H from the glass substrate because of the differences in speed of flow), we normalize the light intensity for each DNA molecule by the average light intensity per pixel for the whole image, and called it the normalized integrated intensity. This completes step two, the determination of the normalized integrated intensity of each ROI, that is, each DNA molecule.

The third step is accomplished by finding the largest separation distance between any two pixels contained in the same ROI (same DNA molecule). This distance is the DNA stretch length. We plot the normalized integrated intensity of the DNA molecule vs its stretch length; see Fig. 5. We found that the normalized intensity fluctuates around a constant for both H = 1 μm and 10 μm positions. For the more coiled stretched DNA molecules, whose stretch lengths are short, the intensity is more scattered than for the stretched molecules. The narrow focal depth apparently causes the larger varia-

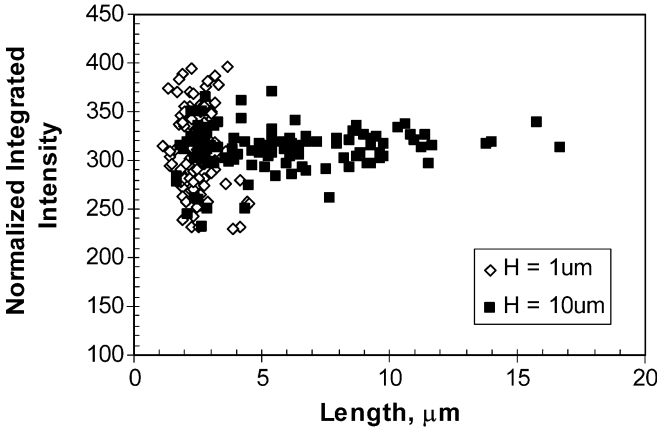

Fig. 5 The normalized integrated intensity vs stretch length of each λ-phage DNA molecule at positions of 1 μm (*open squares*) and 10 μm (*solid diamonds*) away from the solid surface

tion in the integrated intensity of coiled DNA molecules, which can be partially out of focus. Overall, the normalized integrated intensity does not correlate with stretch length of the DNA, and it is on average the same for molecules both near the surface ($H = 1$ μm) and in the bulk ($H = 10$ μm); see Fig. 5. This indicates that the reduced stretching in the nearsurface region is not the result of molecular breakage or other artifact that would produce either a correlation between stretch (i.e., length of the object) and brightness or a difference in DNA brightness between the near-surface and bulk regions.

DNA stretching near/on APTES-coated glass surfaces

We studied DNA stretching in a shearing flow in which the lower glass surface was coated with APTES. The coating chemistry is depicted in Fig. 6. Hydroxyl groups are exposed on the surface after concentrated-acid cleaning, and the hydroxyl in APTES reacts with that on the glass surface and generates a water molecule. DNA molecules will be negatively charged at pH > 7 and be attracted to the positively charged amine groups at the surface (Wingard et al. 1976) due to the entropy gain from release of counterions.

We then studied the stretch of DNA on the APTES-coated lower glass surface in steady shearing flow. We took images at different radial positions every 10 min (some of these images are shown in Fig. 7) and analyzed these images to obtain the time-dependent molecular deposition rate, average stretch $< x >$, and average orientation parameter $S = 2\left(\left\langle \cos^2 \alpha \right\rangle - \frac{1}{2}\right)$ of the molecules at different Wi. The orientation angle $\alpha(-90° \le \alpha \le 90°)$ is defined as the angle between the radial direction and the molecule's longest stretching direction.

On the APTES-coated surface, DNA molecules were irreversibly absorbed after stretching in the flow (the

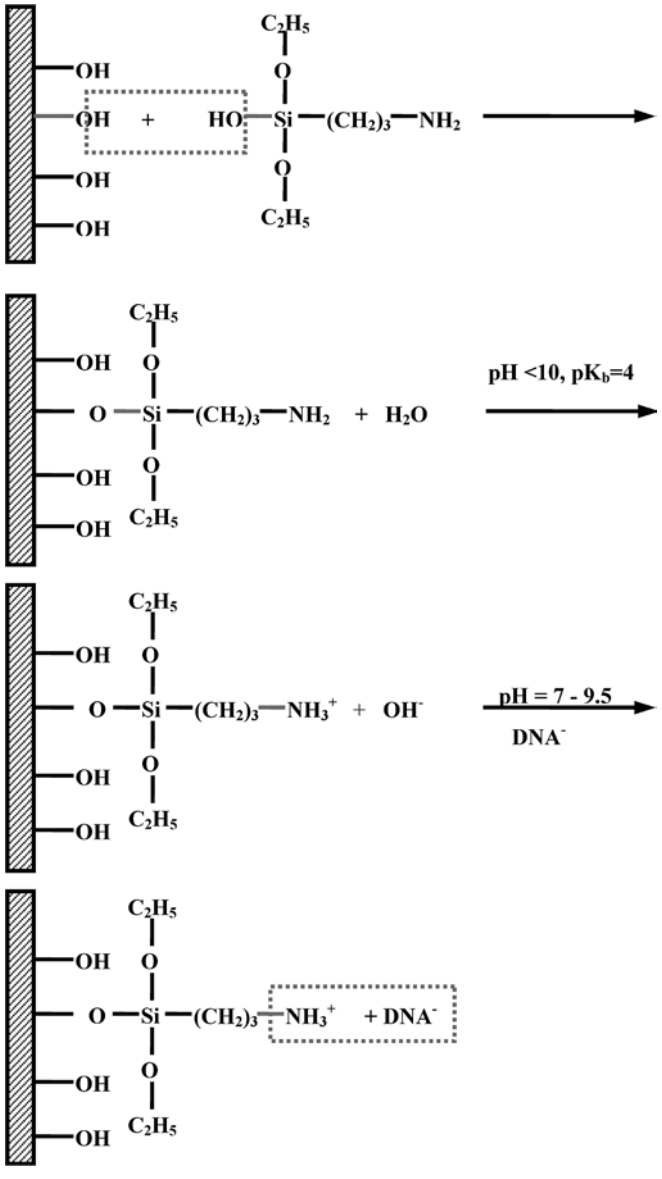

Fig. 6 APTES surface coating mechanism. At pH < 10, the APTES coating is positively charged, while at pH near neutral, DNA is negatively charged and binds strongly to APTES coating

molecules might also stretch as they are adsorbing onto the surface). We find that the average stretch $< x >$ (in Fig. 8c) is much less than in the bulk. The average stretch also reaches a plateau value at much lower Wi than that in the bulk (as shown in Fig. 2). Figure 8a shows that the deposition rate is constant initially, and then the surface coverage begins to level off. (Even with the slow-down in deposition, the molecular number density is not uniform over the viewing field of the microscope, which covers an area of 85×67 μm^2. This indicates that the APTES treatment might not produce a uniformly coated surface.) The orientation parameter (Fig. 8b) at time zero indicates that the molecules are

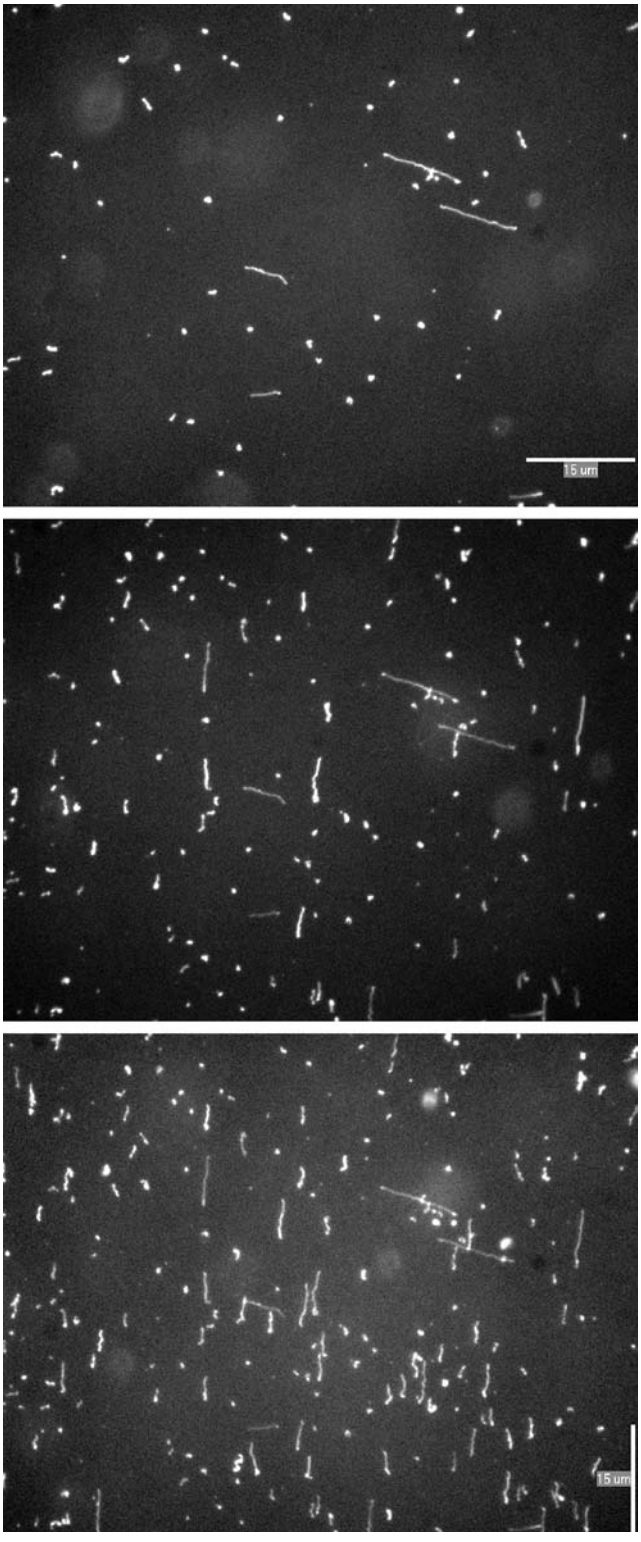

Fig. 7a,b DNA images on an APTES-coated glass coverslip at different times in a torsional shearing flow at $Wi = 14$: **a** $t = 0$, just after depositing the DNA solution onto the surface and mounting the upper plate; **b** $t = 60$ min; **c** $t = 120$ min after startup of shearing. The *scale bar* is 15 μm. The flow is in the vertical direction

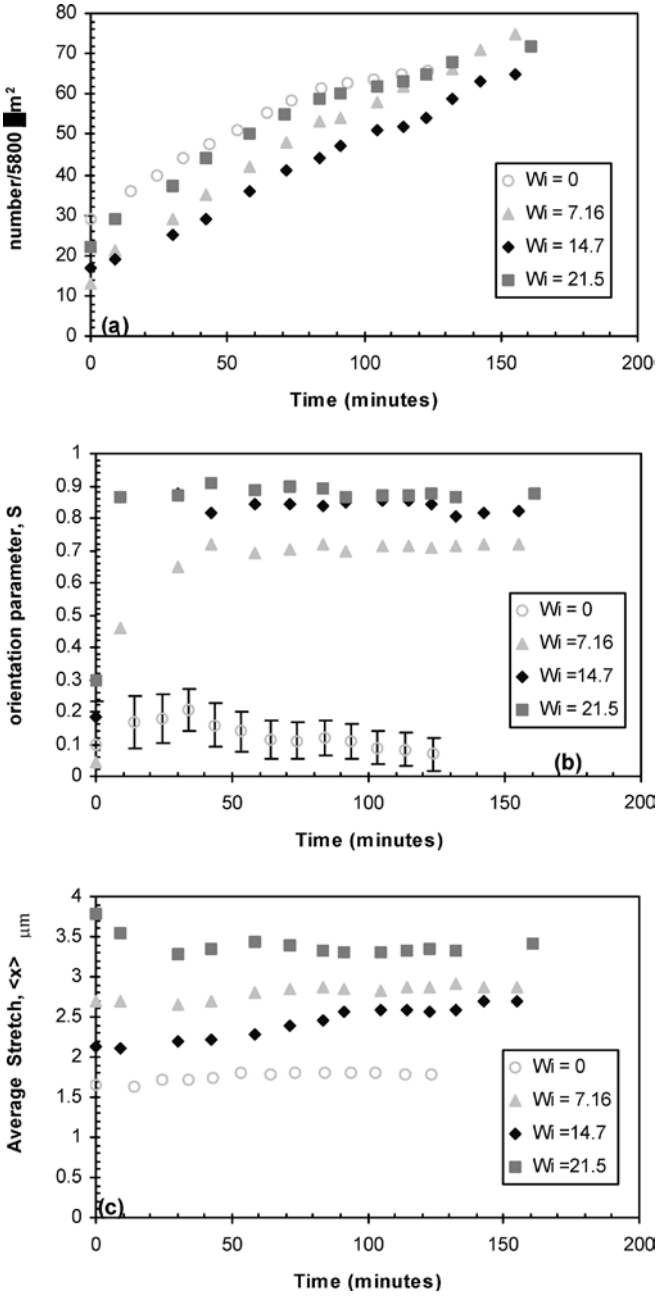

Fig. 8 **a** Density of DNA molecules deposited on an APTES-coated surface vs time. **b** DNA molecular orientation parameter S vs time. Except for the points at zero time, the first image has been subtracted from subsequent images, and all subsequent data is a running average that accumulates with time. **c** Average length $< x >$ vs time, again as a running average with the first image subtracted

mostly randomly oriented with an orientation parameter of around zero when they are first deposited on the surface before the shearing flow starts. As shearing starts and continues, more oriented molecules are deposited on the surface and the orientation parameter S approaches 0.9 for Wi in the range of 14∼20.

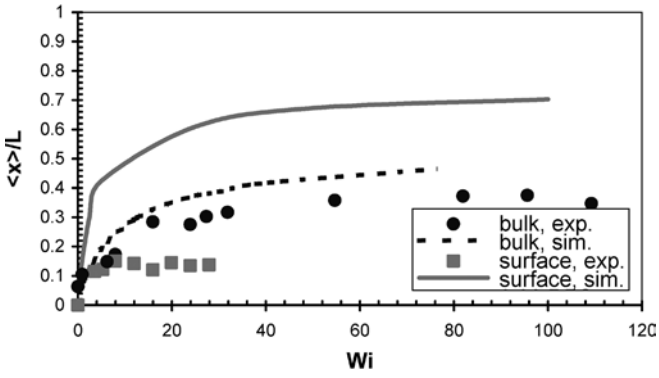

Fig. 9 Comparisons between simulations (*lines*) and experiments (*symbols*). *Closed circles* are experimental measurements of average stretch ratio $< x/L >$ for DNA molecules in the bulk solution under shearing flow, and *squares* are for molecules adsorbed on the surface, The *solid and dashed lines* are predictions of the Brownian dynamics simulations for chains at the surface and in the bulk respectively. The experimental conditions of the shearing flow are the same as in Fig. 2

Comparison between experimental and simulation results

Brownian dynamics simulations have been performed of DNA deposition from bulk solution in a steady simple shearing flow onto an adsorbing surface (Chopra and Larson 2002), with no adjustable parameters, and we now compare our experimental results for the average stretch ratio, $< x/L >$, with these simulation results both in the bulk and on the surface. Apparently, although the simulation can predict the DNA average stretch ratio fairly well in the bulk solution as seen the filled circles and dotted line in Fig. 9 (Li and Larson 2000a; Hur et al. 2000; Chopra and Larson 2002), the simulations predict much higher stretch on the surface (solid line in Fig. 9) than in the bulk (dashed line), while the experiments measure much less stretch on the surface (filled squares in Fig. 9) than in the bulk (filled circles). This discrepancy in stretch of adsorbed chains is similar to that found for chains in the near-wall region. As mentioned previously (see Fig. 4), the experimental measurements show that in a large region near the wall (up to about one third of the molecular contour length, that is, up to 22 μm for T2-phage DNA) the average stretch is significantly reduced below that of the bulk, while the simulations show that the region where the stretch is affected by the wall is less then a micron. Hence, to resolve these disparities between experimental and simulation results, future work should focus on surface characteristics and near-surface flow behavior.

Conclusions

In this work, λ-phage and T2-phage DNA molecules have been used to study macromolecular behavior near adsorbing and non-adsorbing solid surfaces under flow.

In a torsional steady simple shear flow, we confirmed the results obtained in bulk shearing flow by Smith et al. (1999), but discovered that DNA molecular stretching is reduced from that observed in the bulk over a surprisingly large region close to the solid surface, namely a region that extends up to one third of L, the fully-extended, or contour, length of the DNA molecule. This result was obtained for two different DNA molecules, T2 DNA (with $L = 67$ μm) and λ-phage DNA (with $L = 21$ μm). The stretch of the molecules adsorbed onto the surface is quite limited; the average stretch x is only 3.5 μm for λ-phage DNA even at a relatively high shear rate, $Wi \approx 21.5$, which is a much smaller stretch than in the bulk at high Wi.

The experimental measurements have been compared with Brownian dynamics simulation results in a simple steady shearing flow (Chopra and Larson 2002). While the simulation results correctly predict the average stretch of DNA molecules in the bulk, they greatly over-predict the stretch on the surface and in the near-surface region. Further investigation should focus on the near-surface region in steady shear flow.

Acknowledgement The authors thank UM B.S. graduate Iphigenia G Karagiannis for helping with the DNA experiments and data analysis. Manish Chopra provided results from Brownian dynamics simulations. The work was supported by NASA Micro-gravity grant NAG32134 and NSF grant CTS-9987402.

References

Abramchuk SS, Khokhlov AR, Iwataki T, Oana H, Yoshikawa K (2001) Direct observation of DNA molecules in a convection flow of a drying droplet. Europhys Lett 55(2):294–300

Allemand JF, Bensimon D, Jullien L, Bensimon A, Croquette V (1997) pH-dependent specific binding and combing of DNA. Biophys J 73:2064–2070

Babcock HP, Smith DE, Hur JS, Shaqfeh ESG, Chu S (2000) Relating the microscopic and macroscopic response of a polymeric fluid in a shearing flow. Phys Rev Lett 85(9):2018–2021

Babcock HP, Teixeira RE, Hur JS, Shaqfeh ESG, Chu S (2003) Visualization of molecular fluctuations near the critical point of the coil-stretch transition in polymer elongation. Macromolecules 36:4544–4548

Bensimon A, Simon A, Chiffaudel A, Croquette V, Heslot F, Bensimon D (1994) Alignment and sensitive detection of DNA by a moving interface. Science 265:2096–2098

Bensimon D, Simon AJ, Croquette V, Bensimon A (1995) Stretching DNA with a receding meniscus—experiments and models. Phys Rev Lett 74(23):4754–4757

Cai WW, Jing JP, Irvin B, Ohler L, Rose E, Shizuya H, Kim UJ, Simon M, Anantharaman T, Mishra B, Schwartz DC (1998) High-resolution restriction maps of bacterial artificial chromosomes constructed by optical mapping. Proc Natl Acad Sci 95:3390–3395

Chopra M, Larson RG (2002) Brownian dynamics simulations of isolated polymer molecules in shear flow near adsorbing and nonadsorbing surfaces. J Rheol 46(4):831–862

Chopra M, Li L, Hu H, Burns MA, Larson RG (2003) DNA molecular configurations in an evaporating droplet near a glass surface. J Rheol 47(5):1111–1132

Doi M, Edwards SF (1986) The theory of polymer dynamics. Oxford Science, Oxford

Doyle PS, Bibette J, Bancaud A, Viovy JL (2002) Self-assembled magnetic matrices for DNA separation chips. Science 295(5563):2237–2237

Gad S, Aurias A, Puget N, Mairal A, Schurra C, Montagna M, Pages S, Caux V, Mazoyer S, Bensimon A, Stoppa-Lyonnet D (2001) Color bar coding the BRCAI gene on combed DNA: a useful strategy for detecting large gene rearrangements. Gene Chromosome Canc 31(1):75–84

Han J, Craighead HG (2000) Separation of long DNA molecules in a microfabricated entropic trap array. Science 288(5468):1026–1029

Han J, Turner SW, Craighead HG (1999) Entropic trapping and escape of long molecules at submicron size constriction. Phys Rev Lett 83(8):1688–1691

Hsieh C, Li L, Larson RG (2003) Modeling hydrodynamic interaction in Brownian dynamics simulations of extensional flows of dilute solutions of DNA and polystyrene. J Non-Newtonian Fluid Mech 113:149–191

Hu H, Larson RG (2002) Measurement of wall-slip-layer rheology in shear-thickening wormy micelle solutions. J Rheol 46(4):1001–1021

Hu J, Wang M, Weier HUG, Frantz P, Kolbee W, Ogletree DF, Salmeron M (1996) Imaging of single extended DNA molecules on flat (aminopropyl)triethoxysilane-mica by atomic force microscopy. Langmuir 12:1697–1700

Hur JS, Shaqfeh ESG, Larson RG (2000) Brownian dynamics simulations of single DNA molecules in shear flow. J Rheol 44:713

Jendrejack RM, Dimalanta ET, Schwartz DC, Graham MD, de Pablo JJ (2003) DNA dynamics in a microchannel. Phys Rev Lett 91(3):Art No 038102

Jing JP, Reed J, Huang J, Hu XH, Clarke V, Edington J, Housman D, Anantharaman TS, Huff EJ, Mishra B, Porter B, Shenker A, Wolfson E, Hiort C, Kantor R, Aston C, Schwartz DC (1998) Automated high resolution optical mapping using arrayed, fluid-fixed DNA molecules. Proc Natl Acad Sci 95:8046

Klein DCG, Gurevich L, Janssen JW, Kouwenhoven LP, Carbeck JD, Sohn LL (2001) Ordered stretching of single molecules of deoxyribose nucleic acid between microfabricated polystyrene lines. Appl Phys Lett 78(16):2396–2398

Larson RG, Perkins TT, Smith DE, Chu S (1997) Hydrodynamics of a DNA molecule in a flow field. Phys Rev E 55:1794–1797

Larson RG, Hu H, Smith D, Chu S (1999) Brownian dynamics simulations of a DNA molecule in an extensional flow field. J Rheol 43:267

Li L, Larson RG (2000a) Comparison of Brownian dynamics simulations with microscopic and light-scattering measurements of polymer deformation under flow. Macromolecules 33(4):1411–1415

Li L, Larson RG (2000b) Excluded volume effects on the birefringence and stress of dilute polymer solutions in extensional flow. Rheol Acta 39:419–427

Li L, Larson RG, Sridhar T (2000) Brownian dynamics simulation of dilute polystyrene solutions. J Rheol 44(2):291–323

Michalet X, Ekong R, Fougerousse F, Rousseaux S, Schurra C, Hornigold N, van Slegtenhorst M, Wolfe J, Povey S, Beckmann JS, Bensimon A (1997) Dynamic molecular combing: stretching the whole human genome for high-resolution studies. Science 277:1518–1523

Pecora R (1991) DNA: a model compound for solution studies of macromolecules. Science 251:893–898

Perkins TT, Smith DE, Chu S (1997) Single polymer dynamics in an elongational flow. Science 276:2016–2021

Pernodet N, Samuilov V, Shin K, Sokolov J, Rafailovich MH, Gersappe D, Chu B (2000) DNA electrophoresis on a flat surface. Phys Rev Lett 85(26):5651–5654

Quake SR, Babcock H, Chu S (1997) The dynamics of partially extended single molecules of DNA. Nature 388:151–154

Schwartz DC, Li XJ, Hernandez LI, Ramnarain SP, Huff EJ, Wang YK (1993) Ordered restriction maps of *Saccharomyces cerevisae* chromosomes constructed by optical mapping. Science 262:110–114

Smith DE, Chu S (1998) Response of flexible polymers to a sudden elongational flow. Science 281:1335

Smith DE, Babcock HP, Chu S (1999) Single-polymer dynamics in steady shear flow. Science 283:1724

Wingard LB, Katchalski-Katzir E, Goldstein L (1976) Applied biochemistry and bioengineering. Vol 1. Immobilized enzyme principles. Academic Press, New York

Yokota H, Sunwoo J, Sarikaya M, van den Engh G, Aebersold R (1999) Spin-stretching of DNA and protein molecules for detection by fluorescence and atomic force microscopy. Anal Chem 71(19):4418–4422